Dynamic network structure of interhemispheric coordination

Karl W. Doron[a], Danielle S. Bassett[b,c], and Michael S. Gazzaniga[a,c,1]

Departments of [a]Psychological and Brain Sciences and [b]Physics, and [c]Sage Center for the Study of the Mind, University of California, Santa Barbara, CA 93106

This contribution is part of the special series of Inaugural Articles by members of the National Academy of Sciences elected in 2011.

Contributed by Michael S. Gazzaniga, September 21, 2012 (sent for review August 5, 2012)

Fifty years ago Gazzaniga and coworkers published a seminal article that discussed the separate roles of the cerebral hemispheres in humans. Today, the study of interhemispheric communication is facilitated by a battery of novel data analysis techniques drawn from across disciplinary boundaries, including dynamic systems theory and network theory. These techniques enable the characterization of dynamic changes in the brain's functional connectivity, thereby providing an unprecedented means of decoding interhemispheric communication. Here, we illustrate the use of these techniques to examine interhemispheric coordination in healthy human participants performing a split visual field experiment in which they process lexical stimuli. We find that interhemispheric coordination is greater when lexical information is introduced to the right hemisphere and must subsequently be transferred to the left hemisphere for language processing than when it is directly introduced to the language-dominant (left) hemisphere. Further, we find that putative functional modules defined by coherent interhemispheric coordination come online in a transient manner, highlighting the underlying dynamic nature of brain communication. Our work illustrates that recently developed dynamic, network-based analysis techniques can provide novel and previously unapproachable insights into the role of interhemispheric coordination in cognition.

community detection | network dynamics | split-brain | temporal network | neural oscillations

The field of split-brain research began several decades ago with the use of a drastic surgical solution for intractable epilepsy (1–3): the severing of the corpus callosum. This procedure significantly decreased the connectivity between the hemispheres, thereby irrevocably altering interhemispheric communication. Although a few interhemispheric pathways remained through subcortical structures and the anterior commissure, examination of callosal function using split visual field experiments clearly demonstrated its role in interhemispheric communication (2). The callosal projection plays a particularly crucial role in a variety of sensory-motor integrative functions of the two hemispheres (4), shows changes with age, and demonstrates the potential for dynamic changes with training (5). In fact, experiments in patients with severance of the callosum revealed that it subserves a large range of behaviors and cognitive functions that underlie the varied workings of the mind.

Interhemispheric communication has been studied using two basic approaches. The first uses behavioral experiments to examine cognitive phenotypes, and the second uses neuroscientific experiments to examine brain phenotypes. Split-brain research initially focused on the former: Patients demonstrated striking behavioral phenotypes that provided clues regarding the underlying mechanics of brain communication. For example, although most perceptual processing appears to be isolated in each hemisphere following surgery, some attentional and emotional mechanisms initiated in one hemisphere can still be communicated to the other, cortically disconnected, hemisphere (6).

Complementing behavioral experiments, neuroscientific studies provided measurements of both functional and anatomical properties of the callosal body (7–11). For example, to understand the functional role of the callosum, electrophysiological recordings in animals were used to characterize the spatial and temporal properties of interhemispheric cross-talk between homologous regions of visual cortex. Subsequent studies further demonstrated that functional coherence, as measured by oscillatory synchronization, is mediated by corticocortical connections passing through the corpus callosum. This interhemispheric communication facilitates the binding of features within and between the visual hemifields (12).

Complementing examination of the functional role of the corpus callosum, anatomical studies demonstrated that the callosum can be divided along its anteroposterior axis into regions with distinct projection topographies (13). These regions differ in terms of their axon density, their size, and the myelination of projections. Such variations in callosal microstructure relate to the type of information being transferred within a given callosal region (14, 15). Large, heavily myelinated fibers allow for rapid interhemispheric integration of primary sensory-motor information, whereas finer, less myelinated fibers allow for intrahemispheric consolidation of more complex multimodal information before interhemispheric communication. Conceivably, smaller fibers that delay interhemispheric communication might reduce interference from conflicting signals and allow for the segregated processing of information within task-specialized hemispheres.

Neuroimaging and Network Theory

The relatively recent development of a host of novel noninvasive neuroimaging techniques has facilitated the examination of interhemispheric connectivity at a much larger spatial scale than was previously possible. Functional [functional MRI, EEG, and magnetoencephalography (MEG)] and structural [MRI and diffusion tensor imaging (DTI)] neuroimaging methods can be used to examine the functional and structural connectivity between hemispheres, respectively. Noninvasive diffusion imaging of the intact brain has identified the strength and density of interhemispheric communication fibers in beautiful detail, potentially providing us with unique information about the targets and function of callosal projections. Studies combining DTI and behavioral measures have demonstrated a relationship between callosal microstructure and task performance under a range of cognitive and perceptual conditions (16–18). Indeed, individual differences in callosal organization might profoundly affect the information integration between the hemispheres (2, 19).

Collectively, these neuroimaging techniques have underscored the large-scale interconnectedness of the human brain in general and the unique connection pathways mediated by the corpus callosum in particular. Recent advances in mathematics, sociology, and physics have provided a means to characterize such connection patterns quantitatively as networks in which nodes represent

Author contributions: K.W.D. designed research; K.W.D. performed research; D.S.B. contributed new reagents/analytic tools; K.W.D. and D.S.B. analyzed data; and K.W.D., D.S.B., and M.S.G. wrote the paper.

The authors declare no conflict of interest.

Freely available online through the PNAS open access option.

[1]To whom correspondence should be addressed. E-mail: m.gazzaniga@psych.ucsb.edu.

This article contains supporting information online at www.pnas.org/lookup/suppl/doi:10.1073/pnas.1216402109/-/DCSupplemental.

brain regions and edges represent connections between those regions (20–29). Network science provides a novel and potentially critical framework in which to understand interhemispheric communication at the scale of large interconnected areas.

In this paper, we illustrate the potential of combining noninvasive neuroimaging techniques with new analytical methods derived from network theory to provide insight into the mechanisms underlying interhemispheric communication. Using a split visual field experiment, we examine brain activity measured using MEG in healthy subjects processing lexical stimuli. By determining the correlated oscillatory activity between sensors over short time intervals, we quantify the dynamic evolution of interhemispheric connectivity during task processing. We conclude by suggesting that the application of dynamic network theory to neuroimaging data might be important for the future of brain research in a world where split-brain patients are no longer available to science.

Split Visual Field Experiment

Here, we focus on an important functional hemispheric asymmetry in humans: language. To probe the role of interhemispheric coordination in language processing, we use a split visual field experiment with lexical stimuli and examine dynamic network structure in oscillatory brain activity in the two visual field conditions.

In nine healthy individuals, we measured continuous brain activity using MEG. Data were sampled at 512 Hz. Experimental trials consisted of a target stimulus composed of either a word (50%) or a "word-like" nonword (50%) (i.e., pseudoword). Experimental trials were randomly presented in the left visual field (LVF) or in the right visual field (RVF). Participants attended covertly to the stimulated visual field and responded via key press to indicate if they saw a word or a pseudoword.

This type of split visual field experiment can isolate an important behavioral phenotype suggestive of interhemispheric communication. When the stimulus is presented in the RVF, where visual information is directed to the language-dominant left hemisphere, individuals more accurately identify the stimulus as a word or pseudoword. In contrast, when the stimulus is presented in the LVF, where visual information is directed to the right hemisphere, individuals less accurately identify the stimulus. The neuroanatomical basis of the RVF advantage might stem from a cortical region in the left occipitotemporal sulcus that encodes the abstract form of visual letter strings as words (30). The RVF advantage might therefore result from degraded orthographic information transferred from the right hemisphere or, alternatively, from the left-right asymmetry of attention that has been a result of the Western reading style (31). A recent study investigating attentional capture with nonlinguistic stimuli supports the role of differential oscillatory sampling mechanisms for the two hemispheres (32).

Spatiotemporal Interhemispheric Communication

Interhemispheric communication likely occurs through the synchronized oscillatory activity of widely distributed brain regions (33). The anatomical locations of these regions might depend on the type of information being processed. Indeed, evidence from partial split-brain patients suggests that callosal transfer of somatosensory information occurs between regions of posterior cortex (34–36), whereas the transfer of other higher level cognitive information might occur between more anterior regions of temporal and frontal cortex (37).

Anatomically distinct interhemispheric processing streams are thought to be associated with frequency-specific synchronization. For example, evidence suggests that the processing of visual information employs underlying α-band oscillations (38), whereas the processing of higher level cognitive information might be coordinated by other frequencies. The interactions between these high- and low-frequency bands are thought to play an important role in neuronal computation and communication (39). Importantly, the frequency specificity of communication is also modulated by connection length. Long interhemispheric communication is thought to be associated with low-frequency oscillatory activity (40), whereas more local processing has been linked to high-frequency activity. At an even larger scale, low-frequency brain rhythms might enable the dynamic evolution of whole-brain networks at behavioral time scales (41, 42).

Taken together, these results suggest that successful interhemispheric transfer of the information necessary to perform our split visual field experiment accurately depends on a combination of oscillatory activity in multiple frequency bands and across distributed networks of brain areas.

Dynamic Network Construction

An exhaustive assessment of frequency-specific communication patterns is outside the scope of the present study. Instead, we focus on a frequency band that has been shown to facilitate spatial attention and enable information transfer between the cerebral hemispheres (43, 44): the low-frequency amplitude envelope of α-band activity. The amplitude envelope correlation (AEC) (45) between pairs of MEG sensors can be used to examine whole-brain coordination potentially associated with information transfer. An estimate of functional connectivity, the AEC is a measure of intersensor association computed over trials that is sensitive to the task-related coupling of visual areas (46), to long-range interactions, and to relationships among different frequencies (45).

To examine dynamic changes in AEC during lexical processing, we construct whole-brain functional connectivity networks as a function of time (*Materials and Methods*). In the following sections, we examine the organization of these temporal networks in the two experimental conditions (LVF and RVF).

Results

Behavioral Evidence for the RVF Advantage. Behavioral results for accuracy confirmed the RVF advantage for lexical stimuli. Paired t tests for proportion correct revealed a significant difference for stimulus condition, RVF (mean = 0.81, SD = 0.06) and LVF (mean = 0.72, SD = 0.07) [$t(8) = 5.28$, $P = 0.0007$, right-tailed]. Paired t tests for response latency did not show significant differences for stimulus condition, RVF (mean = 568.83, SD = 78.22) and LVF (mean = 543.72, SD = 78.07) [$t(8) = 1.8$, $P = 0.10$, right-tailed]. Given the emphasis in this particular experiment on the speed of response, we did not expect to find statistically significant differences in response latencies in the two experimental conditions.

Interhemispheric Network Coordination. We investigated dynamic interhemispheric coordination and lateralization during presentation of a lexical stimulus in either the LVF or RVF. Lexical stimuli presented in the LVF are subsequently transferred via the corpus callosum to the language-dominant left hemisphere (Fig. 1*A*). To study this transfer, we focused on the interhemispheric elements of the weighted network W. To quantify the differences in interhemispheric connectivity between the two experimental conditions (LVF and RVF), we computed the set of binary networks $\mathbf{B}^{\mathrm{L}>\mathrm{R}}$ and $\mathbf{B}^{\mathrm{R}>\mathrm{L}}$ across the 500-ms poststimulus interval whose nonzero elements were those connections that had significantly different weights in the two conditions. We quantified the extent of condition-dependent interhemispheric connectivity using the network densities of $\mathbf{B}^{\mathrm{R}>\mathrm{L}}$ and $\mathbf{B}^{\mathrm{L}>\mathrm{R}}$, defined as the percentage of edges with significantly different weights in the two conditions (*Materials and Methods*).

We observed differences in network density between stimulus presentations in the two visual fields as a function of time. Compared with the RVF, the LVF stimulus showed pronounced and greater network density at two distinct peaks (100 ms and 300 ms), indicating critical points of interhemispheric coordination that might facilitate the transfer of information from the right hemisphere to the left hemisphere (Fig. 2). One could hypothesize that the first peak reflects the recognition of visual word forms (in posterior areas) and the second peak reflects the retrieval of lexical information (stored in temporal cortex), although this hypothesis would need to be supported by future studies. Network edges are topographically arranged in a way that is suggestive of multiple routes of interhemispheric coordination.

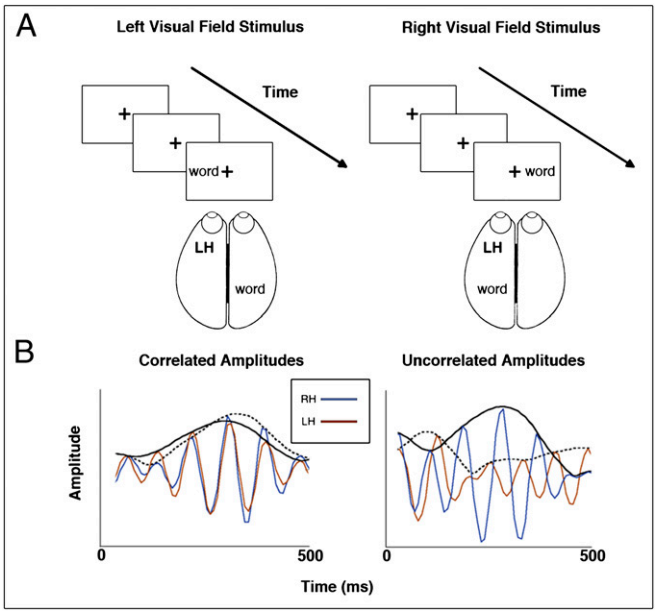

Fig. 1. (*A*) Stimulus presentation and design. The schematic shows the LVF and RVF stimulus conditions. In each condition, a lexical stimulus comprising a word or pseudoword was randomly presented to the subject for 100 ms. Lexical stimuli presented to the RVF are processed directly by the left hemisphere (LH). Neural representations of a stimulus presented to the LVF must be transferred through the corpus callosum to the language-dominant LH for processing. (*B*) MEG signals extracted from the α-band (8–12 Hz). Schematics show correlated (*Left*) and uncorrelated (*Right*) pairs of signals from an LH sensor (brown) and a right hemisphere (RH) sensor (blue). Solid black and dashed lines depict the amplitude envelope for the LH and RH signals, respectively. Note that we computed the correlation between amplitude envelopes across trials at each time point.

For example, sensor-sensor connections are seen for direct left hemisphere and right hemisphere interactions as well as between posterior sensors and frontal sensors of the contralateral hemisphere. The physical locations of these interactions suggest coordination via subcortical structures, such as the thalamus.

We also observed a substantial number of interhemispheric connections in the RVF condition despite the lack of an obvious need for interhemispheric transfer of lexical information to the language-dominant left hemisphere. These connections might instead facilitate other cognitive functions, for example, by enabling the right hemisphere's involvement in directing spatial attention to both visual fields (47, 48). Additionally, the network density for the RVF stimulus presentations increases late in the poststimulus period (400–500 ms) relative to the LVF presentations (Fig. 2*B*), suggesting the involvement of higher order cognitive processes relevant to language that unfold over a longer time course (49).

Dynamic Community Structure. The spatial distribution of interhemispheric connections shown in Fig. 2 suggests that brain function might be facilitated by the coordinated activity of functional modules that span the two hemispheres and that these modules might differ between the two experimental conditions (LVF and RVF). To identify putative functional modules in a robust, data-driven fashion and to explore their temporal evolution during the experiment, we apply recently developed dynamic community detection techniques (50–52). Following previous work (41, 42, 53), we constructed multilayer networks for each individual experimental condition and trial in which we link the weighted network A for each time window t to the network in the time windows before $(t - 1)$ and after $(t + 1)$ (Fig. 3*A*) by connecting each node to itself in the neighboring windows (*Materials and Methods*). We optimize the modularity quality function (52, 54, 55) of these multilayer networks to partition the set of MEG sensors into time-dependent putative functional modules containing groups of sensors with strongly correlated amplitude envelopes of α-band activity.

We observe that the community structure shows different interhemispheric coordination patterns at distinct time points during each stimulus condition (Fig. 3*A*). In particular, we note that communities appear to show differing degrees of lateralization that might be indicative of the hemispheric asymmetry of language processing (56). To quantify these effects, we define a laterality index (LI) that measures the degree to which a community is largely interhemispheric ($LI \approx 0$) or lateralized to one hemisphere or the other ($LI \approx 1$) (*Materials and Methods*). We find that interhemispheric community structure is organized along an anterior-posterior gradient (Fig. 3 *B* and *C*). We therefore define laterality indices for frontal (LI_f), central (LI_c), and posterior (LI_p) sensor regions separately.

Community lateralization in frontal sensors was consistently observed across participants and in both stimulus conditions (results from a representative subject are presented in Fig. 3*A*). Under both stimulus conditions, there is a general and contrasting trend for posterior interhemispheric coordination (i.e., low LI_p) and frontal lateralization (i.e., high LI_f). This trend is evident early in the LVF stimulus condition and late in the RVF stimulus condition, as shown by the shaded regions in Fig. 3*C*. We quantified these observations by performing permutation tests between the LI of paired sensor regions across stimulus conditions (e.g., LVF LI_p vs. RVF LI_p). These tests reveal significant differences in the laterality of frontal sensors at distinct time points. In the LVF condition, LI_f shows greater lateralization during the first 150 ms (i.e., for time points 1–4) [LVF LI_f: mean = 0.82, SD = 0.26; RVF LI_f: mean = 0.70, SD = 0.28; $t \approx 2.35$, $P \approx 0.039$). By contrast, LI_f in the RVF condition shows greater lateralization for the last 150 ms (i.e., for time points 7–11) (LVF LI: mean = 0.55, SD = 0.33; RVF LI: mean = 0.80, SD = 0.28; $t \approx 2.77$, $P \approx 0.017$, one-tailed). Significant differences in laterality were not found at any time point for comparisons between central sensors for the two conditions (LVF LI_c and RVF LI_c) or for posterior sensors for the two conditions (LVF LI_p and RVF LI_p).

Discussion

Historical Context. The dynamic coordination of the two brain hemispheres, mediated by connections through the corpus callosum, is essential for a unified experience of the world (57). Historically, questions surrounding interhemispheric communication have relied primarily on indirect behavioral measures in patients undergoing callosotomy. Before such research, the complete severing of the corpus callosum had surprisingly little observable effect on the behavior of these patients in the real world. Not until Gazzaniga et al. (1) tested the patients using lateralized procedures did we come to appreciate the full extent to which the two hemispheres are specialized for different functions. This separation of function implies that ongoing cognitive and perceptual processing is dynamically integrated between specialized brain modules.

New methods from across scientific disciplines are uncovering the complex interactions that might give rise to the unified experience of the mind (58, 59). In the present study, we combine neuroimaging techniques with network theory to quantify interhemispheric coordination robustly. We used sensor-sensor amplitude correlations of neural oscillatory activity in the α-band recorded with MEG to determine how this coordination changes over time. Our results indicate that network characteristics of interhemispheric coordination during lexical processing depend on whether the stimulus was presented to the left or right brain hemisphere. Further, they suggest that interhemispheric coordination occurs at distinct time points in each stimulus condition and in distinct sets of brain regions along an anterior-posterior axis. The dynamic nature of these effects suggests these methods provide potential access to the spatiotemporal coding mechanisms of the brain.

Neuroimaging and Dynamic Network Analysis. Network theory has been used to examine functional and structural brain connectivity over the past several years (20–29). Examination of MEG

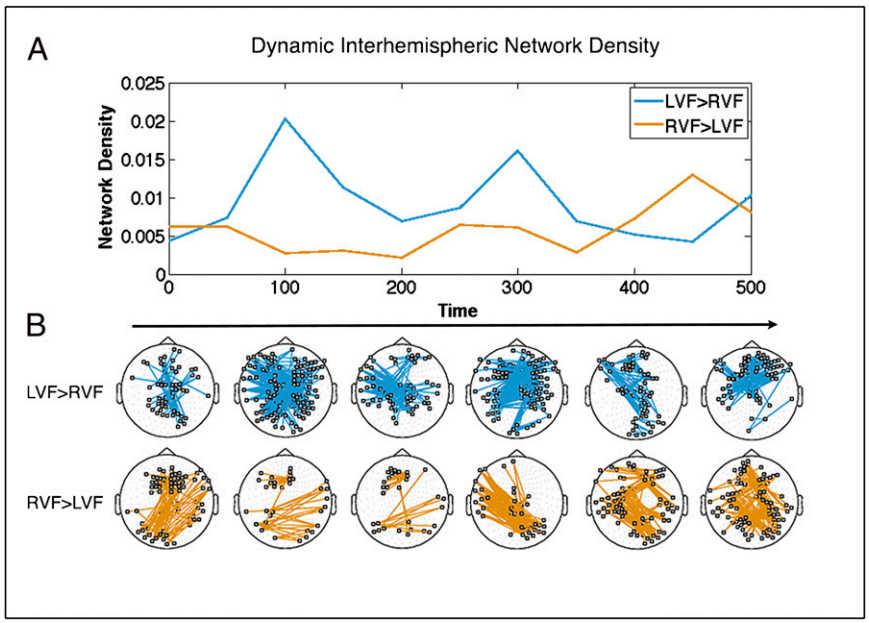

Fig. 2. Poststimulus dynamic interhemispheric network density. Filtered signals at each trial were baseline-corrected by a 500-ms intertrial interval. The correlations between interhemispheric pairwise signal amplitudes in the α-band were used to construct a weighted sensor-sensor network. Subsequent permutation testing was performed (n = 1,000) over participants to determine which connections were stronger in the LVF (LVF > RVF) condition and which were stronger in the RVF (RVF > LVF) condition. (*A*) Network density for each permutation test. Network density is defined as the sum of suprathreshold connections [e.g., LVF > RVF at $P < 0.01$, family-wise error rate (FWER)-corrected] divided by the total number of possible connections. (*B*) Topography of poststimulus connections for each permutation test. Dynamic changes in interhemispheric connections are evident over time, with two visible peaks in the LVF > RVF condition, indicating relatively early times of greater interhemispheric coordination when a lexical stimulus is presented in the LVF.

data using these techniques has demonstrated that functional brain network organization is a biologically meaningful phenotype being altered in disease states (25) in ways that can be linked to behavioral task performance (60–62). Moreover, network organization demonstrates temporal variability that can be induced by cognitive remediation strategies (63), task practice (64), learning (41, 53, 65), or task difficulty (66).

In this study, we explore the use of dynamic network analysis to probe interhemispheric coordination in the highly lateralized function of language processing. Our results demonstrate the powerful nature of the dynamic network methodology, which parsimoniously represents a large number of functional interactions using global network-based signatures like density and community structure. In addition, we use a mathematical definition of network laterality to quantify the lateralization of brain connectivity and its evolution during the poststimulus interval statistically. This quantity will likely be of use in a variety of other more general network science contexts in which putative functional modules can be subdivided into two distinct groups (e.g., gender identification in social networks).

Importantly, network techniques can be successfully complemented by alternative analytical approaches. Dynamic causal modeling, for example, has been used to provide complementary insights into the role of transcallosal coupling (67) in related lateralization effects (68, 69) by estimating the effective connectivity rather than the functional connectivity between regions of interest. Indeed, the choice of connectivity estimate is an open one (21), and different measures of association might provide additional information regarding transfers occurring in other frequency bands (70, 71).

Dynamic Changes in Interhemispheric Coordination. Our results suggest that the extent and anatomical specificity of interhemispheric coordination is time-dependent, highlighting the usefulness of dynamic network methods to explore brain function (41, 42, 65). As shown in Fig. 2, sensor-sensor communication, measured using low-frequency AECs of α-band activity, is present between the hemispheres. Furthermore, this communication is modulated by experimental condition: A greater density of interhemispheric connections occurs when a lexical stimulus is presented to the right hemisphere and then transferred to the language-dominant left hemisphere than when it is presented to the left hemisphere immediately. In light of evidence from split-brain patients that the transfer of lexical information is mediated by transcallosal connections (72), these results demonstrate that network density might be an indirect measurement of visual information transfer across the corpus callosum.

Critically, the observed increase in interhemispheric connectivity occurs early in the poststimulus period, supporting its role in the processing of lower level visual information (73). The two peaks in interhemispheric connectivity center around 100 ms and 300 ms, respectively. The early timing of these features is consistent with the transfer of visual information regarding the lexical stimuli, thought to occur in the first few hundred milliseconds poststimulus (74).

We also note that sensor-sensor correlations in both stimulus conditions result in connections that do not appear to be linked directly by known corticocortical routes, for example, those linking frontal sensors in one hemisphere with posterior sensors in the contralateral hemisphere. It is possible that these functional connections are mediated by subcortical structures, including the thalamus, across which interhemispheric communication is thought to occur in the absence of an intact callosum in split-brain patients (2, 75, 76). However, these results must be interpreted cautiously in light of the volume conduction effects of MEG data that make anatomical localization difficult, the intact resting state connectivity in people with agenesis of the corpus callosum (77), and the potential presence of functional connections mediated by indirect structural connectivity (78).

Dynamic Community Structure. To examine putative functional modules facilitating interhemispheric communication, we investigated the dynamic community structure of sensor-sensor correlations. Interhemispheric connections operated along an anterior-posterior gradient, with greater lateralization in frontal regions and greater coordination found between posterior regions. These differences might be explained in terms of the microstructure of the corpus callosum as well as in terms of evolutionary theories of brain lateralization (79–81). In evolutionary terms, the lateralization of function has been described as a means of extending a new function to the opposite hemisphere while still retaining the old function in the original one. These new regions might benefit from reduced interhemispheric connectivity that would otherwise induce noise by imposing unnecessary cross-talk between brain modules.

Interestingly, our results showing relatively reduced functional connectivity between frontal sensors are consistent with anatomical studies demonstrating the presence of smaller diameter, slower conducting transcallosal fibers in callosal subregions with

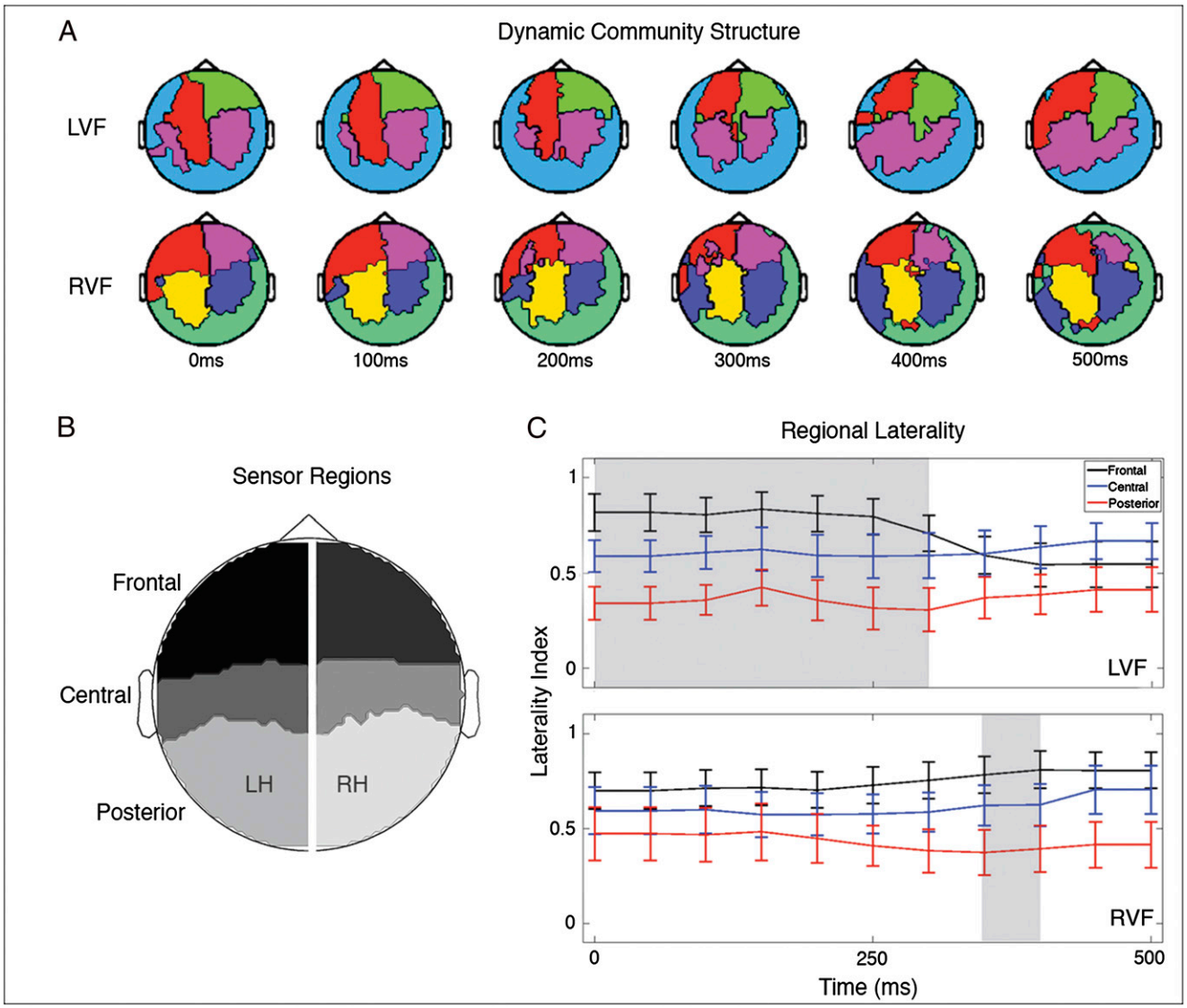

Fig. 3. Dynamic community structure and community laterality. (*A*) Results from a representative participant show the community assignments for each stimulus condition across time. Each colored area represents a community of sensors in which low-frequency amplitudes of the α-band envelope are more correlated within the community than between that community and other communities. We note that qualitatively similar results were found in the remaining participants. (*B*) To study the anatomical locations of communities, we labeled sensors in both the left hemisphere (LH) and right hemisphere (RH) as part of either frontal, central, or posterior regions (depicted by different levels of shading). (*C*) Using the community assignments in *A*, we constructed an *LI* for each set of the left-right sensor regions in *B* for each community at each time point and for each participant (*Materials and Methods*). The LI_f, LI_c, and LI_p sensors averaged over communities are plotted across time. The shaded gray regions show significantly different *LI* values for frontal, central, and posterior sensors at different time points ($P < 0.05$, corrected for multiple comparisons across time). Error bars indicate SEM over subjects. We note that the relatively large error bars in *C* were driven by one participant with particularly low LI_f.

frontal projection topographies (11). The follow-up analysis of regional differences between the stimulus conditions demonstrates significantly greater frontal lateralization during the first 150 ms, when the stimulus is presented in the LVF. In contrast, there is greater frontal lateralization during the last 150 ms, when the stimulus is presented in the RVF. This implies greater interhemispheric coordination (i.e., lower *LI*) in the last 150 ms of the LVF condition and might reflect compensatory involvement of the right hemisphere under the more difficult LVF stimulus condition (82). However, the precise functional role of these differences remains to be clarified.

Methodological Considerations

The present study investigated α-amplitude correlations as a signature of functional brain connectivity. We hypothesized that the transfer of visual word information, potentially modulated by effects of spatial attention, would occur primarily between posterior brain regions of extrastriate cortex. Given the novelty of our approach, we chose to limit our analysis to the α-band, where oscillatory activity has been shown to play a role in similar tasks (83–86). We chose a commonly used α-frequency bandwidth (8–12 Hz), but we note that other studies suggest a functional distinction between the upper and lower α-bands (87). Future studies could therefore investigate the network properties of these distinct bands as well as those of other frequencies (e.g., δ, θ, β, γ) and, furthermore, could determine their function within each hemisphere separately.

In addition to the AEC used here, other oscillatory mechanisms exist that might mediate communication in large-scale brain networks. Oscillatory phase, for example, has been shown to play

a significant role in the communication of large-scale brain systems (88, 89). Phase communication is described in a model in which in-phase oscillations facilitate interaural communication, whereas out-of-phase oscillations suppress it (33). Although the present study was limited to the amplitude envelope, these amplitude peaks appear to oscillate at a frequency below the α-band, suggesting it is possible that the phase of the lower frequency is related to the amplitude of the higher frequency. Indeed, such cross-frequency interactions have been reported in both human and animal studies (90, 91). The role of such interactions in dynamic network states remains an open question.

The α-oscillation has recently been shown to play an inhibitory role in brain function (86, 92). With this in mind, we emphasize the coordination of the hemispheres rather than excitatory connectivity exclusively. The dynamic nature of the results presented here does not preclude functional inhibition; for the LVF stimulus, we find two peaks (100 ms and 300 ms) of coordinated activity that might reflect the correlation of either low amplitudes or high amplitudes between the two hemispheres. The time periods of reduced amplitude correlation might also show an inverse relationship across the hemispheres. For instance, the relative lack of amplitude coordination during the RVF stimulus could indicate inhibition of one hemisphere and excitation of the other. Therefore, it would be interesting in future studies to investigate both amplitude and phase relationships over poststimulus time periods to distinguish the oscillatory mechanisms involved. Finally, the study of oscillatory phase might enhance our understanding of the timing and directionality of brain communication because it allows for the estimation of a region's causal influence on another region.

Conclusion

In this work, we use network analysis techniques that could potentially capture previously hidden oscillatory processes that might prove key to understanding the complex mechanisms underlying cortical-cortical transmission of information. The work reveals a dynamic network evolution more nuanced than originally thought, with putative network signatures of the information-processing phenomenon appearing and disappearing in a given temporal epoch. Through the ability to measure and quantify oscillatory activity with new network analysis techniques, dimensions of the neural processes involved, even in this simple task, can become critical elements of an overall model of information flow in the brain. While the simplicity of the surgical disconnection revealed the presence of complex interhemispheric communication patterns, it did not offer an explanation as to how that interhemispheric communication occurred. We hope these network-based approaches will contribute to a deeper understanding of those processes.

Materials and Methods

Participants. Sixteen right-handed undergraduate students (12 female) recruited from the Otto von Guericke University, Magdeburg, Germany, participated with written consent. The mean age was 20.5 y. All participants were native speakers of German and free of known neurological disorders. The experiment was carried out in accordance with the guidelines of the Ethics Committee of the University of Magdeburg Faculty of Medicine. Participants were paid on a per-hour basis. Experimental sessions lasted ∼150 min. Seven participants' data were excluded due to excessive artifacts or below chance behavioral performance in the LVF stimulus condition.

Data Acquisition and Processing. MEG signals were acquired with a whole-head system with 248-channel dc-magnetometers (BTI Magnes 2500 WH). Signals were corrected for environmental noise by means of a weighted subtraction of reference signals detected by additional sensors close to the superconducting quantum interference device sensors. Participants were seated semireclined in the electromagnetically shielded room ∼100 cm from a backlight projection screen. Head position was maintained by the whole-head MEG equipment and foam pads placed between a participant's head and the equipment. Data were acquired at 512 Hz. The 500-ms poststimulus time segment from each trial was baseline-corrected with a 500-ms intertrial interval. We performed a time frequency analysis to determine the Fourier coefficients for frequencies from 8 to 12 Hz in 1-Hz steps using a sliding window technique (93). Each window contained five cycles and was tapered with a single Hanning window, resulting in a spectral smoothing of roughly 2.5 Hz and a temporal resolution of 25 ms. Amplitude correlations for trial averages at each time point were then computed from the Fourier coefficients using the Fieldtrip software function connectivity_analysis.m (94, 95). This resulted in a single weighted network for each time point and participant from which we selected a network time "slice" every 50 ms. For visualization of the connections and network structure, Figs. 2 and 3 show representations only from every 100 ms.

Experimental Procedures. Stimuli were presented parafoveally at 1.5° of visual angle to the left or right of a central fixation point (cross-hair) so as to direct stimuli to one hemisphere or the other. Participants pressed one of two keys in response to a target that displayed either to the LVF or RVF (uniformly at random) for 100 ms: word (key 1) or pseudoword (key 2). Speed was stressed over accuracy.

Network Construction. To examine whole-brain functional connectivity, we computed an ensemble of weighted networks in which nodes represent MEG sensors and edges between these nodes were weighted by the AEC between all pairwise sensor time series over trials. To examine dynamic changes in AEC during lexical processing, we constructed these networks as a function of time. For each individual, we estimated the sensor-sensor AEC across trials for each time window t to construct a set of T-weighted networks $\{A\}$. Here, $T = 11$ is the number of consecutive, nonoverlapping time windows examined during the 500-ms poststimulus period; a single window was sampled every 50 ms. Each matrix $\mathbf{A}$ in this set contains elements A_{ij} with values equal to the AEC between sensor i and sensor j at a given time point t. A separate set $\mathbf{A}$ was constructed for each participant ($n = 9$), each time point ($n = 11$), and each experimental condition ($n = 2$). Topographical plots in Figs. 2 and 3 show data from every other time point (i.e., every 100 ms) simply for ease of visualization.

Dynamic Interhemispheric Coordination. To study interhemispheric information transfer, we first focused on the interhemispheric elements of the weighted network $\mathbf{A}$ by defining the matrix $\mathbf{W}$ whose elements W_{ij} were equal to A_{ij} if sensor i was in a different hemisphere than sensor j and 0 otherwise. We note that $\mathbf{W}$ is therefore a bipartite network delineating the connections that are present between hemispheres.

To quantify the differences in interhemispheric connectivity between the two experimental conditions (LVF and RVF), we computed the binary network $\mathbf{B}^{L>R}$ whose elements $B_{ij}^{L>R}$ were set to 1 if the weights of that edge W_{ij} were statistically greater in the LVF condition than in the RVF condition and were 0 otherwise. Similarly, we defined the binary network $\mathbf{B}^{R>L}$ whose elements $B_{ij}^{R>L}$ were set to 1 if the weights of that edge W_{ij} were statistically greater in the RVF condition than in the LVF condition and were 0 otherwise. Importantly, to avoid connections along the midline that belong to neither hemisphere, we excluded all possible connections between the 18 sensors along the vertex. This procedure left a potential 115 sensors per hemisphere that could be linked by interhemispheric connections.

Statistically significant differences between the edge weights in the two experimental conditions were determined by permutation testing. We performed a paired samples permutation t test ($n = 9$, 1,000 permutations, $\alpha = 0.05$, right-tailed) with family-wise error rate correction for multiple comparisons (96) between the set of weights for a given edge W_{ij} in the LVF condition and the same edge in the RVF condition. This test was performed on every possible edge connecting the two hemispheres to create a t value and P value for each edge. We used the conservative threshold of $P < 0.01$ to create the binary matrices $\mathbf{B}^{L>R}$ and $\mathbf{B}^{R>L}$, whose elements had a value of 1 if the P value for that edge was less than 0.01 and was 0 otherwise.

We quantified the extent of condition-dependent interhemispheric connectivity using the time-dependent network densities of $\mathbf{B}^{R>L}$ and $\mathbf{B}^{L>R}$, defined as the percentage of edges present at a given time point. The network density for each pairwise comparison (RVF > LVF or LVF > RVF) therefore represented the percentage of significantly different interhemispheric connection weights in the two conditions. Connections common to both experimental conditions are effectively eliminated by the nature of the permutation testing (LVF > RVF) and (RVF > LVF).

Additional comparisons with phase-randomized surrogate data are described in *SI Results*.

Dynamic Community Detection. To determine groups of sensors that show strong AECs with one another, we use community detection tools (51, 50). We first consider the set of L connectivity matrices $\mathbf{A}$ from the 11 time points described in the previous section for each individual. Together, this set forms a rank 3 adjacency tensor A that can be used to represent these time-dependent networks. One can then define a multilayer modularity (52):

$$Q = \frac{1}{2\mu}\sum_{ijlr}\{(|A_{ijl}| - \gamma_l P_{ijl})\delta_{lr} + \delta_{ij}\omega_{jlr}\}\delta(g_{il}, g_{jr}), \quad [1]$$

where the adjacency matrix of layer l has components $|A_{ijl}|$, the element P_{ijl} gives the components of the corresponding matrix for an optimization null model, γ_l is the structural resolution parameter of layer l, g_{il} gives the community assignment of node i in layer l, g_{jr} gives the community assignment of node j in layer r, ω_{jlr} is the connection strength (i.e., a "coupling parameter") between node j in layer r and node j in layer l, the total edge weight in the network is $\mu = \frac{1}{2}\sum_{jr}\kappa_{jr}$, the strength of node j in layer l is $\kappa_{jl} = k_{jl} + c_{jl}$, the intralayer strength of node j in layer l is k_{jl}, and the interlayer strength of node j in layer l is $c_{jl} = \sum_r \omega_{jlr}$. Here, we use a multilayer null model based on the Newman–Girvan null model for single-slice networks (54) by defining

$$P_{ijl} = \frac{k_{il}k_{jl}}{2m_l}, \quad [2]$$

where $k_{il} = \sum_j |A_{ijl}|$ is the strength of node i in layer l and $m_l = \frac{1}{2}\sum_{ij}|A_{ijl}|$. Because we are studying temporal networks, we only couple network slices that are adjacent to one another in time. We note that we focus here on the absolute value of the weighted connectivity matrix **A** to examine the magnitude of interhemispheric coordination irrespective of sign.

We optimize the multilayer quality function Q using a Louvain-like locally greedy algorithm (97). Due to its near-degeneracy (98), we perform 100 optimizations of Q and choose the representative partition of the sensors into communities in a two-step process. First, we calculate the similarity between partitions obtained from different optimizations of Q using the z-score of the Rand coefficient (99). For each pair of partitions α and β, we calculate the Rand z-score in terms of the total number of pairs of nodes in the network M, the number of pairs M_α that are in the same community in partition α, the number of pairs M_β that are in the same community in partition β, and the number of pairs of nodes $w_{\alpha\beta}$ that are assigned to the same community both in partition α and in partition β. The z-score of the Rand coefficient comparing these two partitions is

$$z_{\alpha\beta} = \frac{1}{\sigma_{w_{\alpha\beta}}}w_{\alpha\beta} - \frac{M_\alpha M_\beta}{M}, \quad [3]$$

where $\sigma_{w_{\alpha\beta}}$ is the SD of $w_{\alpha\beta}$. In a second step, we determine which partition is the most similar to all other partitions by calculating which partition has the largest average z-score in comparison to the rest of the partitions. We refer to this partition as the "representative partition" and use it for the remainder of the analysis.

To determine the degree to which a community is largely present in a single hemisphere or bridges both hemispheres, we define a time-dependent network *LI*. For each participant s, each time point t, and each community i, we calculate

$$LI(s,t,i) = \frac{\left|n(s,t,i)^L - n(s,t,i)^R\right|}{n(s,t,i)^L + n(s,t,i)^R}, \quad [4]$$

where $n(s, t, i)^L$ is the number of sensors for participant s, time point t, and community i that are present in the left hemisphere and $n(s, t, i)^R$ is the number of sensors in that same community that are present in the right hemisphere. If a community contains sensors that are only present in one hemisphere, the *LI* will equal 1; if half of the sensors are in one hemisphere and half are in the other hemisphere, the *LI* will equal 0.

To examine community lateralization as a function of the location along the anterior-posterior axis, we further defined the *LI* of frontal, central, and posterior regions (Fig. 3*B*). The lateralization of the frontal region was defined as

$$LI_f(s,t,i) = \frac{\left|n_f(s,t,i)^L - n_f(s,t,i)^R\right|}{n_f(s,t,i)^L + n_f(s,t,i)^R}, \quad [5]$$

where $n_f(s, t, i)^L$ is the number of sensors for participant s, time point t, and community i that are present in the left frontal region and $n_f(s, t, i)^R$ is the number of sensors in that same community that are present in the right frontal region. The lateralization for central LI_c and posterior LI_p regions was defined similarly. Results were averaged over communities to report variations over time and participants (Fig. 3*C*).

ACKNOWLEDGMENTS. We thank Eleanor Brush, Bryan Daniels, Jessica Flack, Mason Porter, and David Krakauer for valuable feedback. This work was supported by the Alexander von Humboldt Foundation, the Errett Fisher Foundation, the Templeton Foundation, the David and Lucile Packard Foundation, Public Health Service Grant NS44393, the Sage Center for the Study of the Mind, and the Institute for Collaborative Biotechnologies through Contract W911NF-09-D-0001 from the US Army Research Office.

1. Gazzaniga MS, Bogen JE, Sperry RW (1962) Some functional effects of sectioning the cerebral commissures in man. *Proc Natl Acad Sci USA* 48:1765–1769.
2. Gazzaniga MS (2005) Forty-five years of split-brain research and still going strong. *Nat Rev Neurosci* 6(8):653–659.
3. Gazzaniga M (2011) Interview with Michael Gazzaniga. *Ann N Y Acad Sci* 1224:1–8.
4. Cisse Y, Grenier F, Timofeev I, Steriade M (2003) Electrophysiological properties and input-output organization of callosal neurons in cat association cortex. *J Neurophysiol* 89(3):1402–1413.
5. Fling BW, Peltier SJ, Bo J, Welsh RC, Seidler RD (2011) Age differences in interhemispheric interactions: Callosal structure, physiological function, and behavior. *Front Neurosci*, 5(38). Available at www.frontiersin.org/Journal/FullText.aspx?d=55&name=&ART_DOI=10.3389/fnins.2011.00038.
6. Corballis MC (1994) Split decisions: Problems in the interpretation of results from commissurotomized subjects. *Behav Brain Res* 64(1–2):163–172.
7. Berlucchi G, Gazzaniga MS, Rizzolatti G (1967) Microelectrode analysis of transfer of visual information by the corpus callosum. *Arch Ital Biol* 105(4):583–596.
8. Berlucchi G, Rizzolatti G (1968) Binocularly driven neurons in visual cortex of split-chiasm cats. *Science* 159(3812):308–310.
9. Berardi N, Bisti S, Maffei L (1987) The transfer of visual information across the corpus callosum: Spatial and temporal properties in the cat. *J Physiol* 384:619–632.
10. Berardi N, Bodis-Wollner I, Fiorentini A, Giuffré G, Morelli M (1989) Electrophysiological evidence for interhemispheric transmission of visual information in man. *J Physiol* 411:207–225.
11. Aboitiz F, Scheibel AB, Fisher RS, Zaidel E (1992) Fiber composition of the human corpus callosum. *Brain Res* 598(1–2):143–153.
12. Engel A, Konig P, Kreiter A, Singer W (1991) Interhemispheric synchronization of oscillatory neuronal responses in cat visual cortex. *Science* 252(5009):1177–1179.
13. Witelson SF (1989) Hand and sex differences in the isthmus and genu of the human corpus callosum. A postmortem morphological study. *Brain* 112(Pt 3):799–835.
14. Aboitiz F, López J, Montiel J (2003) Long distance communication in the human brain: Timing constraints for inter-hemispheric synchrony and the origin of brain lateralization. *Biol Res* 36(1):89–99.
15. Lamantia AS, Rakic P (1990) Cytological and quantitative characteristics of four cerebral commissures in the rhesus monkey. *J Comp Neurol* 291(4):520–537.
16. Genç E, Bergmann J, Singer W, Kohler A (2011) Interhemispheric connections shape subjective experience of bistable motion. *Curr Biol* 21(17):1494–1499.
17. Baird AA, Colvin MK, Vanhorn JD, Inati S, Gazzaniga MS (2005) Functional connectivity: Integrating behavioral, diffusion tensor imaging, and functional magnetic resonance imaging data sets. *J Cogn Neurosci* 17(4):687–693.
18. Westerhausen R, Grüner R, Specht K, Hugdahl K (2009) Functional relevance of interindividual differences in temporal lobe callosal pathways: A DTI tractography study. *Cereb Cortex* 19(6):1322–1329.
19. Häberling IS, Badzakova-Trajkov G, Corballis MC (2011) Callosal tracts and patterns of hemispheric dominance: A combined fMRI and DTI study. *Neuroimage* 54(2):779–786.
20. Bassett DS, Bullmore ET (2006) Small-world brain networks. *Neuroscientist* 12(6):512–523.
21. Bullmore ET, Bassett DS (2011) Brain graphs: Graphical models of the human brain connectome. *Annu Rev Clin Psychol* 7:113–140.
22. Bullmore E, Sporns O (2009) Complex brain networks: Graph theoretical analysis of structural and functional systems. *Nat Rev Neurosci* 10(3):186–198.
23. Sporns O (2010) *Networks of the Brain* (MIT Press, Cambridge, MA).
24. Sporns O (2011) The human connectome: A complex network. *Ann N Y Acad Sci* 1224:109–125.
25. Bassett DS, Bullmore ET (2009) Human brain networks in health and disease. *Curr Opin Neurol* 22(4):340–347.
26. Bullmore E, Sporns O (2012) The economy of brain network organization. *Nat Rev Neurosci* 13(5):336–349.
27. He Y, Evans A (2010) Graph theoretical modeling of brain connectivity. *Curr Opin Neurol* 23(4):341–350.
28. Stam CJ, van Straaten EC (2012) The organization of physiological brain networks. *Clin Neurophysiol* 123(6):1067–1087.
29. Kaiser M (2011) A tutorial in connectome analysis: Topological and spatial features of brain networks. *Neuroimage* 57(3):892–907.
30. McCandliss BD, Cohen L, Dehaene S (2003) The visual word form area: Expertise for reading in the fusiform gyrus. *Trends Cogn Sci* 7(7):293–299.
31. Nicholls ME, Wood AG, Hayes L (2001) Cerebral asymmetries in the level of attention required for word recognition. *Laterality* 6(2):97–110.
32. Landau AN, Fries P (2012) Attention samples stimuli rhythmically. *Curr Biol* 22(11):1000–1004.
33. Fries P (2005) A mechanism for cognitive dynamics: neuronal communication through neuronal coherence. *Trends Cogn Sci* 9(10):474–480.

34. Gazzaniga MS, Freedman H (1973) Observations on visual processes after posterior callosal section. *Neurology* 23(10):1126–1130.
35. Fabri M, et al. (2001) Posterior corpus callosum and interhemispheric transfer of somatosensory information: An fMRI and neuropsychological study of a partially callosotomized patient. *J Cogn Neurosci* 13(8):1071–1079.
36. Ihori N, Kawamura M, Fukuzawa K, Kamaki M (2000) Somesthetic disconnection syndromes in patients with callosal lesions. *Eur Neurol* 44(2):65–71.
37. Arguin M, et al. (2000) Divided visuo-spatial attention systems with total and anterior callosotomy. *Neuropsychologia* 38(3):283–291.
38. Romei V, Gross J, Thut G (2010) On the role of prestimulus alpha rhythms over occipito-parietal areas in visual input regulation: Correlation or causation? *J Neurosci* 30 (25):8692–8697.
39. Canolty RT, Knight RT (2010) The functional role of cross-frequency coupling. *Trends Cogn Sci* 14(11):506–515.
40. von Stein A, Sarnthein J (2000) Different frequencies for different scales of cortical integration: From local gamma to long range alpha/theta synchronization. *Int J Psychophysiol* 38(3):301–313.
41. Bassett DS, et al. (2011) Dynamic reconfiguration of human brain networks during learning. *Proc Natl Acad Sci USA* 108(18):7641–7646.
42. Bassett DS, et al. (2012) Robust detection of dynamic community structure in networks. *arXiv*:1206.4358.
43. Hamm JP, Dyckman KA, McDowell JE, Clementz BA (2012) Pre-cue fronto-occipital alpha phase and distributed cortical oscillations predict failures of cognitive control. *J Neurosci* 32(20):7034–7041.
44. Foxe JJ, Snyder AC (2011) The Role of Alpha-Band Brain Oscillations as a Sensory Suppression Mechanism During Selective Attention. *Front Psychol* 2:154.
45. Bruns A, Eckhorn R, Jokeit H, Ebner A (2000) Amplitude envelope correlation detects coupling among incoherent brain signals. *Neuroreport* 11(7):1509–1514.
46. Bruns A, Eckhorn R (2004) Task-related coupling from high- to low-frequency signals among visual cortical areas in human subdural recordings. *Int J Psychophysiol* 51(2): 97–116.
47. Mesulam MM (1981) A cortical network for directed attention and unilateral neglect. *Ann Neurol* 10(4):309–325.
48. Shulman GL, et al. (2010) Right hemisphere dominance during spatial selective attention and target detection occurs outside the dorsal frontoparietal network. *J Neurosci* 30(10):3640–3651.
49. Bastiaansen MC, van der Linden M, Ter Keurs M, Dijkstra T, Hagoort P (2005) Theta responses are involved in lexical-semantic retrieval during language processing. *J Cogn Neurosci* 17(3):530–541.
50. Fortunato S (2010) Community detection in graphs. *Phys Rep* 486(3–5):75–174.
51. Porter MA, Onnela J-P, Mucha PJ (2009) Communities in networks. *North American Mathematical Society* 56(9):1082–1097, 1164–1166.
52. Mucha PJ, Richardson T, Macon K, Porter MA, Onnela J-P (2010) Community structure in time-dependent, multiscale, and multiplex networks. *Science* 328(5980):876–878.
53. Wymbs NF, Bassett DS, Mucha PJ, Porter MA, Grafton ST (2012) Differential recruitment of the sensorimotor putamen and frontoparietal cortex during motor chunking in humans. *Neuron* 74(5):936–946.
54. Newman MEJ, Girvan M (2004) Finding and evaluating community structure in networks. *Phys Rev E Stat Nonlin Soft Matter Phys* 69(2 Pt 2):026113.
55. Newman MEJ (2004) Fast algorithm for detecting community structure in networks. *Phys Rev E Stat Nonlin Soft Matter Phys* 69(6 Pt 2):066133.
56. Desmond JE, et al. (1995) Functional MRI measurement of language lateralization in Wada-tested patients. *Brain* 118(Pt 6):1411–1419.
57. Sperry R, Gazzaniga M, Bogen J (1969) *Handbook of Clinical Neurology* (North-Holland, Amsterdam), Vol 4, pp 273–290.
58. Doron KW, Gazzaniga MS (2008) Neuroimaging techniques offer new perspectives on callosal transfer and interhemispheric communication. *Cortex* 44(8):1023–1029.
59. Bassett DS, Gazzaniga MS (2011) Understanding complexity in the human brain. *Trends Cogn Sci* 15(5):200–209.
60. Bassett DS, et al. (2009) Cognitive fitness of cost-efficient brain functional networks. *Proc Natl Acad Sci USA* 106(28):11747–11752.
61. Bosma I, et al. (2009) Disturbed functional brain networks and neurocognitive function in low-grade glioma patients: A graph theoretical analysis of resting-state MEG. *Nonlinear Biomed Phys* 3(1):9.
62. Castellanos NP, et al. (2011) Principles of recovery from traumatic brain injury: Reorganization of functional networks. *Neuroimage* 55(3):1189–1199.
63. Weiss SA, et al. (2011) Functional Brain Network Characterization and Adaptivity During Task Practice in Healthy Volunteers and People with Schizophrenia. *Front Hum Neurosci,* 5(81). Available at www.frontiersin.org/Human_Neuroscience/10.3389/fnhum.2011.00081/full.
64. Deuker L, et al. (2009) Reproducibility of graph metrics of human brain functional networks. *Neuroimage* 47(4):1460–1468.
65. Mantzaris AV, et al. (2012) Dynamic network centrality summarizes learning in the human brain. *arXiv*:1207.5047.
66. Kitzbichler MG, Henson RN, Smith ML, Nathan PJ, Bullmore ET (2011) Cognitive effort drives workspace configuration of human brain functional networks. *J Neurosci* 31 (22):8259–8270.
67. Grefkes C, Eickhoff SB, Nowak DA, Dafotakis M, Fink GR (2008) Dynamic intra- and interhemispheric interactions during unilateral and bilateral hand movements assessed with fMRI and DCM. *Neuroimage* 41(4):1382–1394.
68. Stephan KE, Penny WD, Marshall JC, Fink GR, Friston KJ (2005) Investigating the functional role of callosal connections with dynamic causal models. *Ann N Y Acad Sci* 1064:16–36.
69. Stephan KE, Marshall JC, Penny WD, Friston KJ, Fink GR (2007) Interhemispheric integration of visual processing during task-driven lateralization. *J Neurosci* 27(13): 3512–3522.
70. Nikouline VV, Linkenkaer-Hansen K, Huttunen J, Ilmoniemi RJ (2001) Interhemispheric phase synchrony and amplitude correlation of spontaneous beta oscillations in human subjects: A magnetoencephalographic study. *Neuroreport* 12(11): 2487–2491.
71. Jung P, et al. (2012) Spatiotemporal dynamics of bimanual integration in human somatosensory cortex and their relevance to bimanual object manipulation. *J Neurosci* 32(16):5667–5677.
72. Mohr B, Pulvermüller F, Rayman J, Zaidel E (1994) Interhemispheric cooperation during lexical processing is mediated by the corpus callosum: Evidence from the split-brain. *Neurosci Lett* 181(1-2):17–21.
73. Klimesch W, Fellinger R, Freundberger R (2011) Alpha oscillations and early stages of visual encoding. *Front Psychol*, 2(118). Available at www.frontiersin.org/Perception_Science/10.3389/fpsyg.2011.00118/full.
74. Brysbaert M (1994) Interhemispheric transfer and the processing of foveally presented stimuli. *Behav Brain Res* 64(1–2):151–161.
75. Gazzaniga MS, Holtzman JD, Smylie CS (1987) Speech without conscious awareness. *Neurology* 37(4):682–685.
76. Holtzman JD (1984) Interactions between cortical and subcortical visual areas: Evidence from human commissurotomy patients. *Vision Res* 24(8):801–813.
77. Tyszka JM, Kennedy DP, Adolphs R, Paul LK (2011) Intact bilateral resting-state networks in the absence of the corpus callosum. *J Neurosci* 31(42):15154–15162.
78. Honey CJ, et al. (2009) Predicting human resting-state functional connectivity from structural connectivity. *Proc Natl Acad Sci USA* 106(6):2035–2040.
79. Gazzaniga MS (2000) Cerebral specialization and interhemispheric communication: Does the corpus callosum enable the human condition? *Brain* 123(Pt 7):1293–1326.
80. Corballis PM, Funnell MG, Gazzaniga MS (2000) An evolutionary perspective on hemispheric asymmetries. *Brain Cogn* 43(1-3):112–117.
81. Rilling JK, Insel TR (1999) Differential expansion of neural projection systems in primate brain evolution. *Neuroreport* 10(7):1453–1459.
82. Farris EA, et al. (2011) Functional connectivity between the left and right inferior frontal lobes in a small sample of children with and without reading difficulties. *Neurocase* 17(5):425–439.
83. Busch NA, Dubois J, VanRullen R (2009) The phase of ongoing EEG oscillations predicts visual perception. *J Neurosci* 29(24):7869–7876.
84. Hamidi M, Slagter HA, Tononi G, Postle BR (2009) Repetitive Transcranial Magnetic Stimulation Affects Behavior by Biasing Endogenous Cortical Oscillations. *Front Integr Neurosci*, 3(14). Available at www.frontiersin.org/Integrative_Neuroscience/10.3389/neuro.07.014.2009/full.
85. Mathewson KE, Gratton G, Fabiani M, Beck DM, Ro T (2009) To see or not to see: Prestimulus alpha phase predicts visual awareness. *J Neurosci* 29(9):2725–2732.
86. Mazaheri A, Nieuwenhuis IL, van Dijk H, Jensen O (2009) Prestimulus alpha and mu activity predicts failure to inhibit motor responses. *Hum Brain Mapp* 30(6):1791–1800.
87. Klimesch W (1999) EEG alpha and theta oscillations reflect cognitive and memory performance: A review and analysis. *Brain Res Brain Res Rev* 29(2-3):169–195.
88. Pavla S, Pavla PM (2012) Discovering oscillatory interaction networks with M/EEG: challenges and breakthroughs. *Trends Cogn Sci* 16(4):219–230.
89. Saalmann YB, Pinsk MA, Wang L, Li X, Kastner S (2012) The pulvinar regulates information transmission between cortical areas based on attention demands. *Science* 337(6095):753–756.
90. Canolty RT, et al. (2006) High gamma power is phase-locked to theta oscillations in human neocortex. *Science* 313(5793):1626–1628.
91. Lakatos P, Karmos G, Mehta AD, Ulbert I, Schroeder CE (2008) Entrainment of neuronal oscillations as a mechanism of attentional selection. *Science* 320(5872):110–113.
92. Klimesch W, Sauseng P, Hanslmayr S (2007) EEG alpha oscillations: The inhibition-timing hypothesis. *Brain Res Brain Res Rev* 53(1):63–88.
93. Mitra PP, Pesaran B (1999) Analysis of dynamic brain imaging data. *Biophys J* 76(2): 691–708.
94. Rosenberg JR, Amjad AM, Breeze P, Brillinger DR, Halliday DM (1989) The Fourier approach to the identification of functional coupling between neuronal spike trains. *Prog Biophys Mol Biol* 53(1):1–31.
95. Oostenveld R, Fries P, Maris E, Schoffelen JM (2011) FieldTrip: Open source software for advanced analysis of MEG, EEG, and invasive electrophysiological data. *Comput Intell Neurosci* 2011:156869.
96. Blair RC, Karniski W (1993) An alternative method for significance testing of waveform difference potentials. *Psychophysiology* 30(5):518–524.
97. Blondel VD, Guillaume JL, Lambiotte R, Lefebvre E (2008) Fast unfolding of community hierarchies in large networks. *J Stat Mech*, 10.1088/1742-5468/2008/10/P10008.
98. Good BH, de Montjoye YA, Clauset A (2010) Performance of modularity maximization in practical contexts. *Phys Rev E Stat Nonlin Soft Matter Phys* 81(4 Pt 2):046106.
99. Traud AL, Kelsic ED, Mucha PJ, Porter MA (2011) Comparing community structure to characteristics in online collegiate social networks. *SIAM Rev* 53:526–543.